Amyloids of Shuffled Prion Domains That Form Prions Have a Parallel In-Register β-Sheet Structure[†]

Frank Shewmaker,[‡] Eric D. Ross,[§] Robert Tycko,*[,||] and Reed B. Wickner*[,‡]

Laboratory of Biochemistry and Genetics, National Institute of Diabetes and Digestive and Kidney Diseases, National Institutes of Health, Bethesda, Maryland 20892-0830, Department of Biochemistry and Molecular Biology, Colorado State University, Fort Collins, Colorado 80523, and Laboratory of Chemical Physics, National Institute of Diabetes and Digestive and Kidney Diseases, National Institutes of Health, Bethesda, Maryland 20892-0520

Received December 17, 2007; Revised Manuscript Received February 9, 2008

ABSTRACT: The [URE3] and [PSI$^+$] prions of *Saccharomyces cerevisiae* are self-propagating amyloid forms of Ure2p and Sup35p, respectively. The Q/N-rich N-terminal domains of each protein are necessary and sufficient for the prion properties of these proteins, forming in each case their amyloid cores. Surprisingly, shuffling either prion domain, leaving amino acid content unchanged, does not abrogate the ability of the proteins to become prions. The discovery that the amino acid composition of a polypeptide, not the specific sequence order, determines prion capability seems contrary to the standard folding paradigm that amino acid sequence determines protein fold. The shuffleability of a prion domain further suggests that the β-sheet structure is of the parallel in-register type, and indeed, the normal Ure2 and Sup35 prion domains have such a structure. We demonstrate that two shuffled Ure2 prion domains capable of being prions form parallel in-register β-sheet structures, and our data indicate the same conclusion for a single shuffled Sup35 prion domain. This result confirms our inference that shuffleability indicates parallel in-register structure.

[URE3] and [PSI$^+$] are amyloid-based prions (infectious proteins) of the Ure2 and Sup35 proteins, respectively, in the yeast *Saccharomyces cerevisiae* (*1–4*). Ure2p and Sup35p each have an N-terminal prion domain and a C-terminal domain sufficient for their functions in nitrogen regulation and translation termination, respectively (*5, 6*).

Both prion domains are rich in asparagine and glutamine residues, but although there are more than 100 similarly Q/N-rich domains in yeast proteins, only these two and the Rnq1 protein (*7–9*) have been shown to be prions. The Sup35p prion domain also has several peptide repeats reminiscent of the N-terminal region of the PrP protein associated with the mammalian transmissible spongiform encephalopathies. Thus, it was surprising that for both Ure2p (*10*) and Sup35p (*11*), shuffling the prion domain sequence, leaving the amino acid content unchanged, produced sequences which were in each case tested (five examined for each protein) able to form prions in vivo. This result shows that it is the amino acid composition of these prion domains, not their exact sequence, that largely determines their ability to be prions. Of course, sequence was not completely without effect as one in five shuffled sequences from Ure2p or Sup35p was an unstable prion, and the frequency of conversion to the prion form varied somewhat from one shuffled sequence to the next (*10, 11*).

Amyloid is a fibrillar structure comprised of β-sheets in which the β-strands are largely perpendicular to the long axis of the fibrils (*12*; reviewed in ref *13*). Most β-sheet structures of soluble enzymes are antiparallel, with the N-terminus to C-terminus orientation of adjacent chains being opposite. However, parallel β-sheets are also known as is the β-helix structure in globular proteins. Amyloid fibrils having parallel or antiparallel structures have been described previously (*14–24*). In principle, a parallel β-sheet fibril can be in-register, meaning that identical residues are aligned along the long axis of the filament, or out of register by any number of residues (Figure 1).

While the ability to be a prion was found to be insensitive to sequence in the cases of Ure2p and Sup35p, it is clear that sequence is absolutely critical for prion propagation. Heterozygosity for the Met/Val polymorphism in human PrP largely prevents infectious or spontaneous Creutzfeldt-Jakob disease (*25, 26*), and changing a single amino acid can block prion propagation in human cells (*27*) and in yeast (*28*). To explain both the importance of sequence in prion propagation and the insensitivity of prion forming ability to shuffling the amino acid sequence of the prion domain, it was proposed that the amyloids involved must have a parallel in-register β-sheet structure (*29, 30*). If amyloid fibrils were composed of antiparallel β-sheets, β-helices, or out-of-register parallel β-sheets, the sequence specificity of prion (or amyloid)

[†] This work was supported by the Intramural Program of the National Institute of Diabetes and Digestive and Kidney Diseases of the National Institutes of Health.

* To whom correspondence should be addressed. R.B.W.: Bldg. 8, Room 225, NIH, Bethesda, MD 20892-0830; phone, (301) 496-3452; fax, (301) 402-0240; e-mail, wickner@helix.nih.gov. R.T.: Bldg. 5, Room 112, NIH, Bethesda, MD 20892-0520; phone, (301) 402-8272; fax, (301) 496-0825; e-mail, robertty@mail.nih.gov.

[‡] Laboratory of Biochemistry and Genetics, National Institute of Diabetes and Digestive and Kidney Diseases.

[§] Colorado State University.

[||] Laboratory of Chemical Physics, National Institute of Diabetes and Digestive and Kidney Diseases.

10.1021/bi7024589 CCC: $40.75
Published on Web 03/07/2008

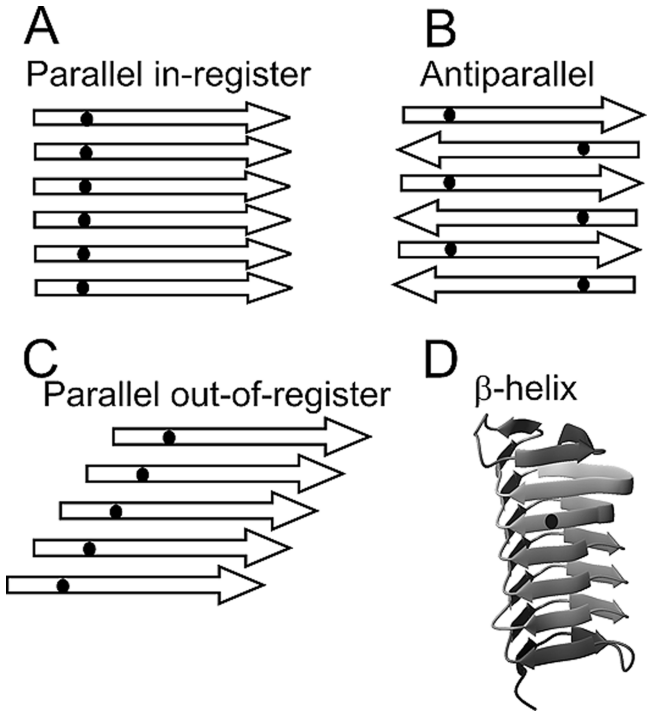

FIGURE 1: Possible β-sheet amyloid structures. Model structures of parallel in-register, parallel out-of-register, antiparallel, and β-helix structures are shown. The β-helix is an antifreeze protein from the spruce budworm *Choristoneura fumiferana* (*49*). The black dot shows the position of a single residue. β-Strands are 0.47 nm apart.

propagation would require some relation between residues aligned in adjacent molecules to explain the stringent sequence specificity in propagation. This relation would almost certainly be destroyed by shuffling the sequence. However, in a parallel in-register β-sheet, identical residues are aligned, and shuffling the sequence would still allow identical residues to align. Thus, a sequence that can be shuffled and still form an amyloid-based prion should make an amyloid with a parallel β-sheet structure.

Indeed, it is known from solid-state NMR[1] data that infectious amyloids of Sup35 and Ure2 prion domains do form parallel in-register β-sheet amyloids (*31, 32*), and analogous experiments using electron spin resonance indicate that an amyloid of PrP has a similar structure (*24*). Here we sought to determine whether the amyloid proteins of shuffled Ure2p and Sup35p prion domains that are capable of forming prions in vivo have a parallel in-register β-sheet structure as predicted.

METHODS

Ure2 Prion Domain Overexpression, Purification, and Filament Formation. All protein expression was performed in fresh transformants of *Escherichia coli* strain BL21-CodonPlus(DE3)-RIPL (Stratagene), and isotopic labeling was achieved using Defined Amino-Acid Medium (DAM) as previously described (*31*).

The expression of Ure2 wild-type and scrambled prion domains was driven from pKT55 (Ure2p$^{M,His6,1-89}$) (*33*) with the wild-type sequence and pER107 (Ure2-21p$^{M,His6,GSQ,1-90}$) and pER110 (Ure2-24p$^{M,His6,GSQ,1-90}$) (*10*) in which residues 1–89 are scrambled with a C-terminal alanine. Following overexpression of Ure2 proteins, cells were pelleted by centrifugation and lysed by vigorous suspension in lysis buffer [8 M guanidine, 100 mM Tris (pH 8.0), and 150 mM NaCl; ~25 mL of lysis buffer per liter of culture] and incubation at room temperature without agitation for approximately 1 h. The lysates were cleared by high-speed centrifugation (~70000*g*). For purification of the tagged Ure2 proteins, the cleared lysates were incubated with nickel−nitrilotriacetic acid (Ni−NTA; ~2 mL per liter of culture) agarose (Qiagen) at 4 °C. After incubation (~1 h) with lysates, the Ni−NTA agarose was loaded into a column and washed extensively with wash buffer [8.5 M urea, 100 mM sodium phosphate, 10 mM Tris, 150 mM NaCl, and 20 mM imidazole (pH 8)], and the Ure2 proteins were eluted using elution buffer [8.5 M urea, 100 mM sodium phosphate, 10 mM Tris, 150 mM NaCl, and 200 mM imidazole (pH 8)]. For amyloid formation, the purified Ure2 proteins were dialyzed into fibrillization buffer [50 mM sodium phosphate and 300 mM NaCl (pH 8.0)] and incubated for several days at 4 °C. The amyloid fibrils were harvested by centrifugation (~50000*g*), washed multiple times with H_2O, and lyophilized for solid-state NMR analysis.

An expression vector for the scrambled variant SUP35-27 was constructed by amplifying SUP35-27p$^{1-254}$ from pER188 (*11*) with 5′ oligo CACCATGTCGTATCAGGGTTACC and 3′ oligo CTATTAATGGTGATGGTGATGATGACCATCGTTAACAACTTCGTC, adding a C-terminal histidine tag with the reverse primer. This PCR product was cloned into pET101D-TOPO and subcloned by transferring the XbaI−SacI fragment into pET-21(a) (Novagen) cut with the same enzymes. The resulting plasmid, designated pFPS169, encodes Sup35-27, with the first 114 residues scrambled plus the additional C-terminal sequence GHHHHHH. Following the overexpression of Sup35-27NM, cells were harvested and lysed as described above. Likewise, protein lysates were similarly cleared, incubated with NiNTA, and loaded onto a column. The column was washed with 3 column volumes of wash buffer and 2 column volumes of soft wash buffer [50 mM potassium phosphate, 500 mM NaCl, and 20 mM imidazole (pH 6.8)] and eluted with 2 column volumes of soft elution buffer [5 mM potassium phosphate, 150 mM NaCl, 200 mM imidazole (pH 6.8), and protease inhibitors (Roche)]. The eluted Sup35-27NM protein contains partially proteolyzed fragments with the C-terminal histidine tag. However with incubation at 4 °C and light agitation for ~1 week, the full-length protein selectively formed filamentous aggregates that were spun out of the mixture, resulting in a relatively pure sample. For solid-state NMR experiments, the filaments were dried by being lyophilized.

Amorphous aggregates of the scrambled Ure2 and Sup35 proteins were prepared by first dissolving approximately 10 mg of dried filamentous samples in 1 mL of 88% formic acid at room temperature for 1 h. To the dissolved samples was added 9 volumes of cold ethanol, and the samples were incubated at −20 °C for several hours or overnight. The precipitated proteins were spun out of solution (~30000*g*), washed with cold 90% ethanol several times, and dried for solid-state NMR analysis (Figure 3).

[1] Abbreviations: NMR, nuclear magnetic resonance; MAS, magic angle spinning.

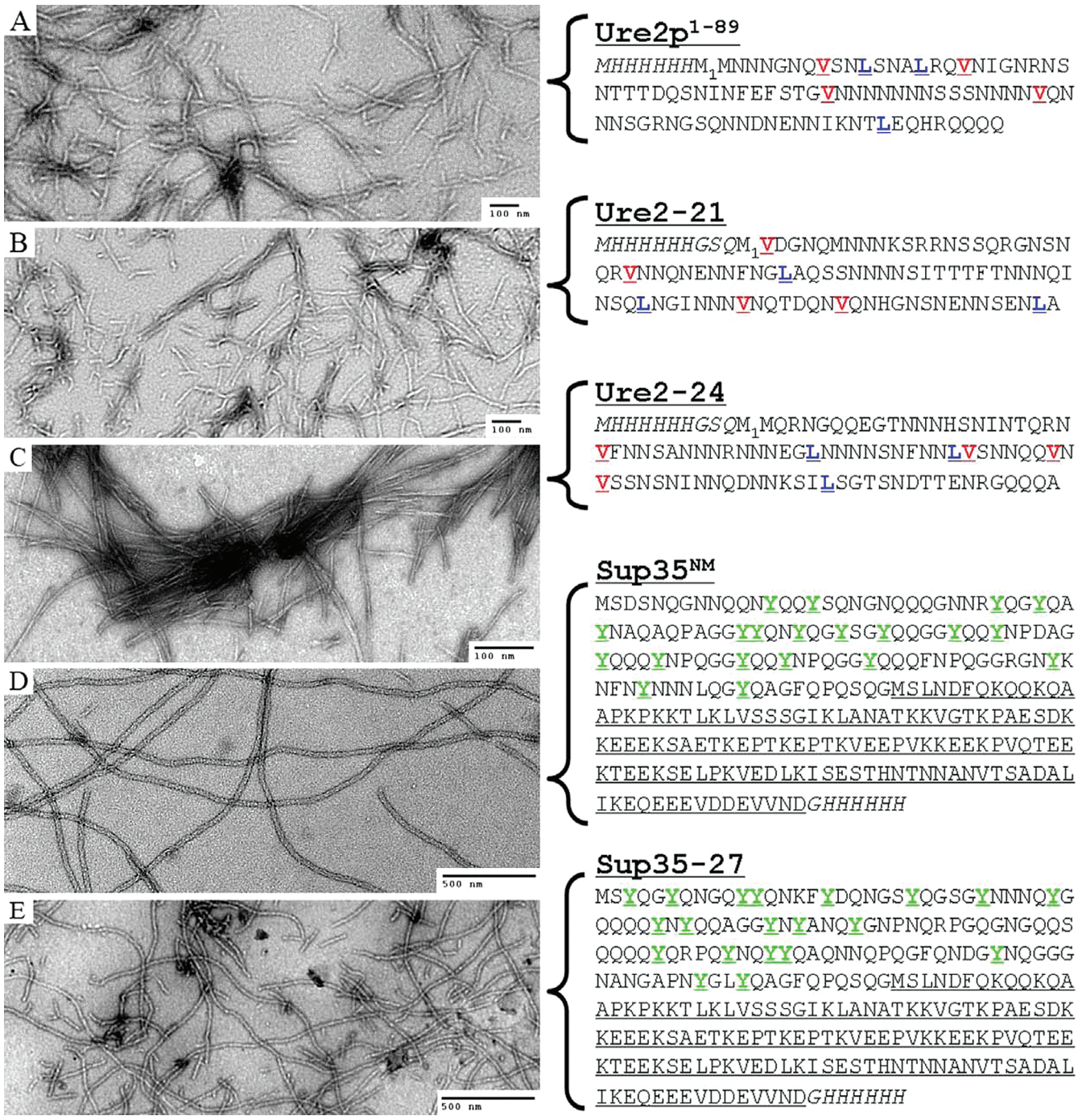

FIGURE 2: Electron micrographs of amyloid filaments of shuffled prion domains of Ure2p and Sup35p: (A) unlabeled Ure2 prion domain, (B) leucine-1-^{13}C-labeled Ure2-21, (C) leucine-1-^{13}C-labeled Ure2-24, (D) unlabeled Sup35NM, and (E) unlabeled Sup35-27. The full amino acid sequence of each purified protein is shown adjacent to the corresponding electron micrograph. The Ure2 variants consist of residues 1–90 and an N-terminal histidine tag. The Sup35 variants consist of resides 1–253 and a C-terminal histidine tag. Colored residues represent sites that were specifically labeled with ^{13}C at the carbonyl position for solid-state NMR experiments. The underlined portion of the Sup35 sequences indicates the unscrambled middle domain.

NMR Methods. Solid-state NMR experiments were carried out at 9.39 T (100.4 MHz ^{13}C NMR frequency) using an InfinityPlus spectrometer (Varian, Palo Alto, CA) and MAS NMR probes (Varian) with 3.2 mm diameter rotors. All measurements were taken at room temperature. ^{13}C NMR spectra were recorded at an MAS frequency of 20.00 kHz with ^{1}H−^{13}C cross-polarization (*34*) and two-pulse phase-modulated ^{1}H decoupling (*35*). The PITHIRDS-CT measurements were carried out at a MAS frequency of 20.00 kHz as described previously (*36*). Pulsed spin-lock detection was used for an improved signal-to-noise ratio (*37*). Each PITHIRDS-CT data point is the result of 576 or more scans with a 4 s recycle delay.

The original PITHIRDS-CT data, $S_{raw}(t)$, were corrected for the 1.1% natural abundance of ^{13}C as follows. (i) PITHIRDS data were recorded for unlabeled samples of Ure2p$^{1-89}$, Ure2-21p$^{1-90}$, and Ure2-24p$^{1-90}$ (Figure 4A,C,D), and the signals decayed to 69, 96, and 77%, respectively (average of 81%), of their initial values by the end of the 76.8 ms recoupling period. Assuming linear decay, the

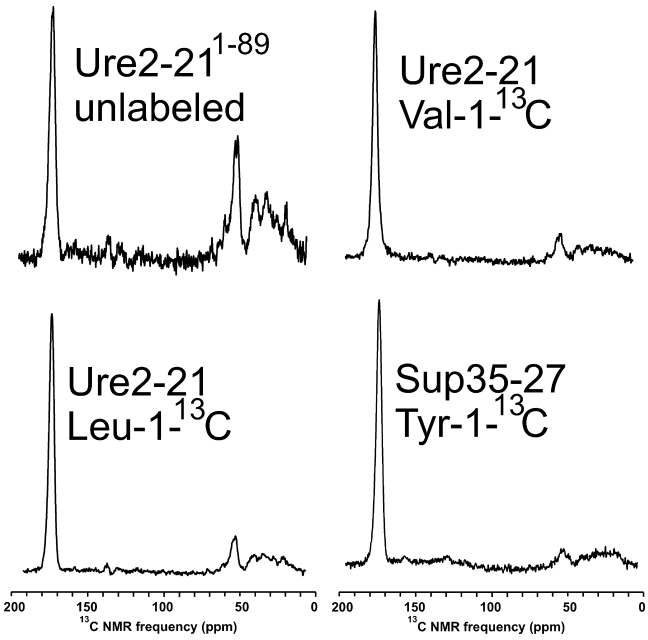

FIGURE 3: Solid-state NMR spectra. Spectra of amyloid of the Ure2-21 prion domain unlabeled or labeled with Leu-1-^{13}C or Val-1-^{13}C or Sup35-27NM labeled with Tyr-1-^{13}C were recorded at 9.39 T and 20 kHz MAS. The carbonyl peak of the Leu-1-^{13}C-labeled sample was asymmetric and could be deconvoluted into two Gaussian peaks.

natural abundance signal is $S_{na} = 100 - 0.25t$, where t is the effective dipolar dephasing time in milliseconds. (ii) The number of natural abundance ^{13}C nuclei per Ure2p$^{1-89}$ or Sup35NM molecule, N_{na}, is 0.011 × (number of total sites − number of labeled nuclei), where the number of total sites is 142 or 339 carbonyls, respectively. The number of labeled nuclei, N_{label}, was 3, 4, and 20 for Leu, Val, and Tyr, respectively, the first two in Ure2$^{1-89}$ and the last in Sup35NM. The corrected PITHIRDS data were as follows: $S(t) = [S_{raw}(t) - f_{na}S_{na}(t)]/(1 - f_{na})$, where $f_{na} = N_{na}/(N_{na} + N_{label})$ and $S_{raw}(0) = 100$. Sup35-27NM data were further corrected for the presence of two pairs of adjacent Tyr residues, whose signal should decay rapidly regardless of the distance from Tyr residues in other molecules. Standard errors are given.

Electron Microscopy. The formation of filaments by shuffled and wild-type proteins was confirmed by electron microscopy of negatively stained samples. A fibril suspension was applied to a carbon-coated copper grid for ∼2 min, washed breifly with H_2O, stained for ∼2 min with 2% uranyl acetate, blotted, and air-dried. The stained samples were examined with an FEI Morgagni transmission electron microscope operating at 80 kV.

RESULTS

Filaments Formed by Shuffled Prion Domains. Among the shuffled Ure2 prion domains, we chose to study the Ure2-21 and Ure2-24 prion domains because they produced the most stable prions at the highest frequencies (*10*) and Sup35-27 because it had the fewest adjacent Tyr residues (four) of the shuffled Sup35 proteins (*11*). Preparations of prion domains of Ure2 (wild type), Ure2-21, and Ure2-24 and the NM segments of Sup35 (wild type) and Sup35-27, incubated as described in Methods, each formed aggregates that were examined by electron microscopy (Figure 2). Sup35NM and Sup35-27NM both formed long, smooth, round, and unbranched filaments ∼10 nm in diameter. Compared to Sup35NM, the prion domains of Ure2, Ure2-21, and Ure2-24 formed shorter filaments with smaller diameters (∼3–6 nm). The Ure2 filaments were also unbranched but tended to stick together and frequently associated laterally. Further, some of the Ure2 filaments had a ribbonlike quality making them look flatter and less round than the Sup35NM filaments. An obvious twist could be seen in such filaments. Overall, there were no obvious differences between filaments formed by the wild-type proteins and the sequence-scrambled variants.

One-Dimensional NMR Spectra Indicate β-Sheet Formation. β-Sheet formation results in a shift of the resonant frequency of carbonyl carbons of 1–3 ppm to lower values (*38–40*). Amyloid filaments of the Ure2 prion domain, and two shuffled versions, Ure2-21 and Ure2-24, each labeled with Leu-1-^{13}C, exhibited major carbonyl peaks at 173.0, 173.0, and 172.8 ppm, respectively, compared to the random coil value of 175.9 ppm (*41*). Amyloid filaments of shuffled Sup35-27NM labeled with Tyr-1-^{13}C had a carbonyl peak at 173.0 ppm, compared to the random coil value of 174.2 ppm. This indicates that each filament preparation was rich in β-sheet.

Dipolar Recoupling NMR Experiments Indicate Parallel In-Register β-Sheet Structure. β-Sheet structures include (i) antiparallel sheets, the most common in globular proteins, in which adjacent strands run in opposite directions (Figure 1), (ii) parallel sheets with adjacent strands running in the same direction, (iii) β-helices, a coil whose strands are in β-configuration, or (iv) hybrid structures, with, for example, some neighboring strands parallel and others antiparallel to each other. Parallel sheets can be in-register, with identical residues aligned, or out-of-register. These different structures predict dramatically different results in our NMR experiments.

If a molecule is carbonyl-^{13}C-labeled at a single amino acid residue, the nearest neighbor ^{13}C is in another molecule. In a parallel in-register β-sheet, this distance is 0.48 nm, namely the same amino acid residue in the preceding and following molecules in the same β-sheet (Figure 1A). In an antiparallel structure, most carbonyl ^{13}C labels will be no closer than 0.96 nm (Figure 1B). In a singly labeled β-helix, the next nearest ^{13}C would probably be many-fold the distance (0.48 nm) between two β-strands, and the precise distance would be determined by the intermolecular orientation (Figure 1D). With several scattered residues labeled (3–20 per molecule in our experiments), if most exhibit a nearest neighbor distance of ∼0.5 nm, the parallel in-register structure is likely. Antiparallel β-sheets are ruled out if multiple labeled sites all exhibit distances of 0.5 nm, and β-helices are ruled out if the nearest neighbor distances are shown to be intermolecular.

In solution NMR, the anisotropy of the chemical shift (the resonant frequency of a given nucleus) and dipole–dipole interaction (the direct interaction of magnetic nuclei) are averaged out by the rapid molecular motion, producing sharp peaks at the isotropic chemical shift frequency. In solid-state NMR, spinning the entire sample at the "magic angle" (∼54.7°) serves this function. Radiofrequency pulses are then used to (selectively) restore (recouple) the dipole–dipole interaction, which because it is inversely proportional to the

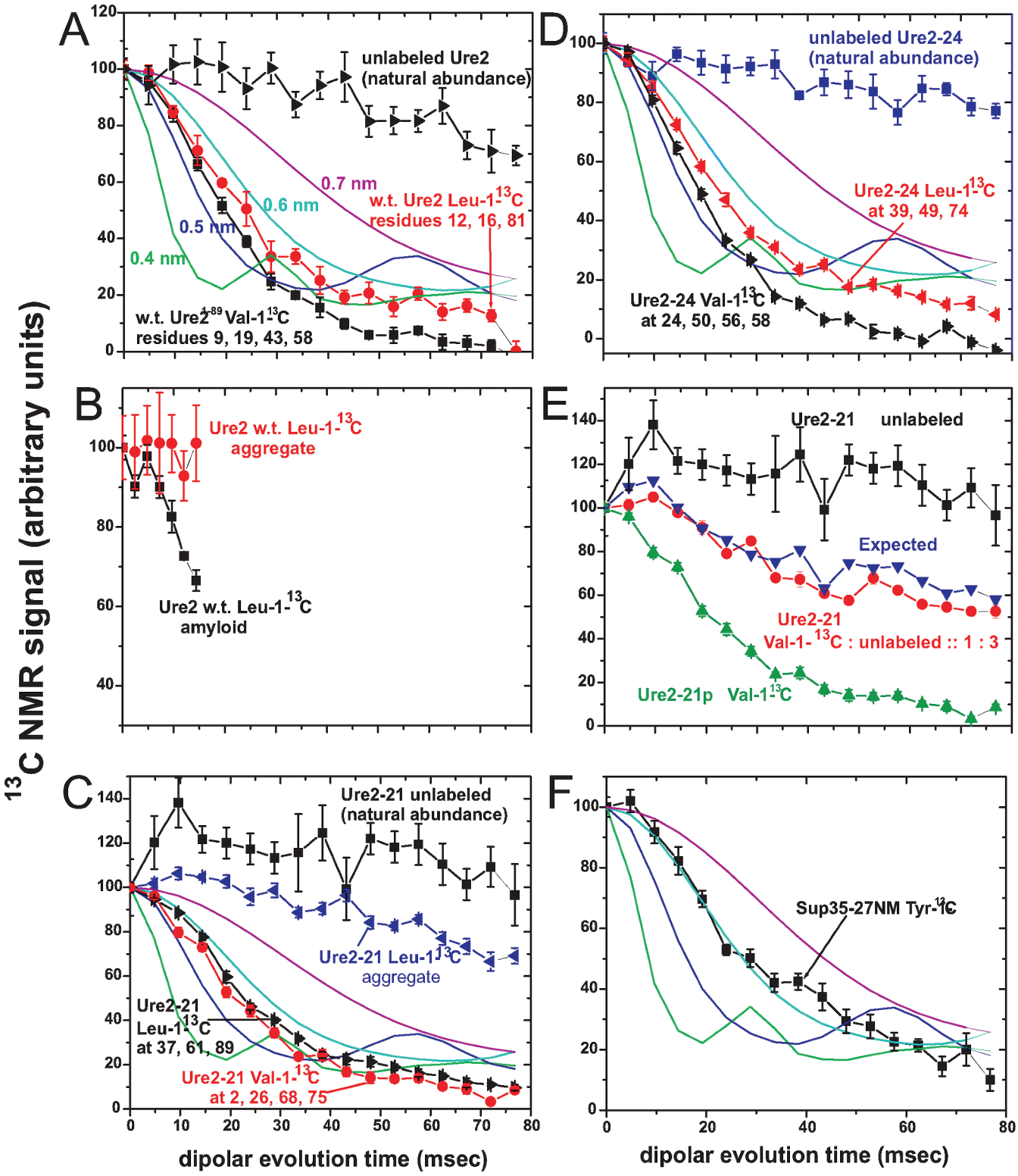

FIGURE 4: Dipolar recoupling experiments indicate parallel structure of shuffled Ure2p and Sup35p prion domains. (A) Dipolar recoupling experiments with Ure2$^{1–89}$ (wild type) unlabeled or labeled with Leu-1-^{13}C or Val-1-^{13}C. The time scale for signal decay is inversely proportional to the cube of the distance to the next nearest ^{13}C. Standard curves for 0.4, 0.5, 0.6, and 0.7 nm are simulations carried out as described previously (*36*). (B) Comparison of signal decay by amyloid of Ure2p$^{1-89}$ Leu-1-^{13}C and a nonspecific aggregate made as described in Methods. Because of the rapid loss of coherence (short T_2) of the aggregate preparation, only a short dipolar evolution time was allowed for both samples. (C) Dipolar recoupling experiments with the Ure2-21 prion domain. (D) Dipolar recoupling experiments with Ure2-24. (E) Diluting Ure2-21 labeled with Val-1-^{13}C with three parts of unlabeled Ure2-21 shows that signal decay is due to intermolecular interactions. The "expected" curve was calculated as $^{9}/_{16}$(Ure2-21 natural abundance) + $^{7}/_{16}$(Ure2-21 Val-1-^{13}C). (F) Dipolar recoupling experiment with Sup35-27NM Tyr-1-^{13}C.

cube of the distance between the interacting dipoles (nuclei with spins) is used to measure distances. Selective labeling of the sample allows the measurement to be targeted to specific residues. The PITHIRDS-CT dipolar recoupling method used here is particularly insensitive to errors in pulse calibration and involves π-pulses lasting one-third of each

rotation period (*36*). A total constant time (hence CT) is occupied by the variable dipolar recoupling period plus a period in which there is no recoupling so that the rate of decay of the NMR signal is primarily a reflection of internuclear distance and is relatively insensitive to spin relaxation (T_2) processes.

As previously shown (*32*), an unlabeled sample of wild-type Ure2p$^{1-89}$, with only the 1.1% natural abundance of ^{13}C and therefore long distances between carbonyl ^{13}C atoms, exhibited very slow decay of the NMR signal (Figure 4A). In contrast, Ure2p$^{1-89}$ labeled with Val-1-^{13}C at residues 9, 19, 43, and 58 showed the rapid signal decay corresponding to a distance between labeled nuclei of ~0.5 nm and indicating a parallel in-register structure (Figure 4A) (*32*). Similar results were found with wild-type Ure2p labeled with Leu-1-^{13}C (residues 12, 16, and 81) (Figure 4A). An ethanol precipitate of formic acid-denatured wild-type Ure2 Leu-1-^{13}C did not exhibit the rapid signal decay, indicating that amyloid structure, not aggregation per se, brings the carbonyl labels close together (Figure 4B).

Shuffled Ure2 prion domains, having the same amino acid content as wild-type Ure2p$^{1-89}$, but any of five completely randomized sequences, were able to form prions in *S. cerevisiae* and amyloid in vitro (*10*). Amyloid formed from one of these, Ure2-21, labeled with either Leu-1-^{13}C (residues 37, 61, and 89) or Val-1-^{13}C (residues 2, 26, 68, and 75), exhibited the same rapid NMR signal decay as wild-type Ure2p, corresponding to an internuclear distance of ~0.5 nm and a parallel in-register β-sheet structure (Figure 4C). A nonspecific aggregate of Leu-1-^{13}C-labeled Ure2-21, formed by solubilization of filaments in formic acid and ethanol precipitation, displayed a slow signal decay, showing that the rapid signal decay was due to the specific amyloid structure, and not simply being an aggregate per se.

A portion of Ure2-21 Val-1-^{13}C monomer was diluted with three parts of unlabeled Ure2-21, and amyloid was formed. If each Val-1-^{13}C were close to another in the same molecule, the rate of signal decay should be unchanged by the dilution. In fact, the signal decayed much slower in the diluted sample than without dilution (Figure 4E), indicating that the nearest neighbor ^{13}C is on a different molecule. The parallel in-register structure predicts that a dilution with three parts of unlabeled Ure2-21 should result in $^3/_4 \times {}^3/_4 = {}^9/_{16}$ of labeled molecules having neither neighboring molecule labeled. The signal decay curve expected on this basis agrees well with the observed results (Figure 4E). In contrast, the β-helix model predicts that most main chain hydrogen bonds would be intramolecular, and so the opposite result in this dilution experiment would be expected.

A second shuffled Ure2 prion domain, Ure2-24, labeled with either Leu-1-^{13}C (residues 39, 49, and 74) or Val-1-^{13}C (residues 24, 50, 56, and 58), likewise exhibited the rapid decay indicative of a parallel in-register β-sheet structure (Figure 4D).

Like the Ure2p prion domain, the prion domain of Sup35p (residues 1–123) can be shuffled and still be capable of prion formation (*11*). One of these shuffled sequences, Sup35-27, with the adjacent unscrambled polar M domain, was labeled with Tyr-1-^{13}C. Amyloid formed with this labeled protein was examined by the same dipolar recoupling experiment described above (Figure 4F). The rate of signal decay reflects an average distance of ~0.6 nm between nearest neighbor Tyr carbonyl carbons. This result suggests a parallel in-register structure for most residues, but with some in turns or loops and giving a slower rate of decay. The result is incompatible with a fully antiparallel or β-helix structure.

DISCUSSION

The prion forming ability of Ure2p and Sup35p has been largely localized to short N-terminal domains (*5, 6*), although other regions of the molecule can affect the frequency of prion generation and the stability of the prions formed (*6, 42, 43*). Surprisingly, the sequence of the prion domains is not critical to prion formation, since for either Ure2p or Sup35p, random shuffling of the residues of the prion domains (five shuffled molecules of each) left the molecule still able to be a prion (*10, 11*). It was inferred that the β-sheets of the amyloid formed by the prion domains must be in a parallel in-register structure (*29, 30*). This inference was verified for wild-type Sup35NM, including the prion domain N and the adjacent polar domain M (*31*). Similar results were found for the prion domain of Ure2p (*32*).

Here we provide evidence that the shuffled prion domains themselves, Ure2-21, Ure2-24, and Sup35-27NM, have the same parallel in-register β-sheet architecture, confirming the inference that shuffleability implies this structure. However, the structures of the various amyloids studied here and previously may have very different lengths and locations of turns and loops, different distant contacts, or different assemblies of protofilaments into fibers within the overall theme of parallel in-register β-sheet structure.

Of course, it has only been shown that Ure2p and Sup35p prion domains can be shuffled and still be prions. This need not be the case for other prions. It is likely that the Q and N "polar zippers", hydrophobic interactions, possible S/T polar zippers, and the low abundance of charged residues in the prion domains of Ure2p and Sup35p determine the parallel in-register β-sheet structure and the shuffleability of these prion domains. It is also possible that some parallel in-register β-sheet prions (amyloids) cannot be shuffled and still be prions (amyloids). Other prions and/or amyloids may form due to specific sequences, or an inability of fibers of shuffled sequences to be fragmented by chaperones may prevent growth from being faster than degradative processes.

To date, except for HETs, all natural amyloids that have been characterized by solid-state NMR or EPR have in-register parallel structure (*18–24*). Some fragments of amyloid-forming proteins form amyloid with antiparallel structure [e.g., Aβ_{34-42} (*14*), Aβ_{16-22} (*40*), and Aβ_{11-25} (*44*)], but none have been proven to have β-helical or out-of-register parallel β-sheet structures. The HETs prion domain (residues 218–289) has two structurally ordered segments that contain β-strands with an imperfect sequence repeat. It has been proposed that these two segments form a parallel β-sheet structure that is "pseudo" in-register, with alignment of similar residues in the two ordered segments. The resulting structure may be considered to be a two-turn β-helix (*45, 46*). Note that HETs is not Q/N-rich, but the parallel in-register pattern is not limited to Q/N-rich amyloids.

Since the parallel in-register architecture appears to be a common basis of most amyloids, it is possible that this may be usable as the basis for therapy of amyloid diseases. While stabilizing the soluble form (reviewed in ref *47*) or reducing

the production of the soluble form (e.g., ref *48*) can each reverse amyloidosis, small molecules that bind to the growing ends of filaments interfering with addition of monomers may also be useful in treatment.

ACKNOWLEDGMENT

We are grateful to Kent Thurber and Kan Hu for many helpful discussions.

REFERENCES

1. Wickner, R. B. (1994) [URE3] as an altered URE2 protein: Evidence for a prion analog in *S. cerevisiae*. *Science 264*, 566–569.
2. King, C. Y., and Diaz-Avalos, R. (2004) Protein-only transmission of three yeast prion strains. *Nature 428*, 319–323.
3. Tanaka, M., Chien, P., Naber, N., Cooke, R., and Weissman, J. S. (2004) Conformational variations in an infectious protein determine prion strain differences. *Nature 428*, 323–328.
4. Brachmann, A., Baxa, U., and Wickner, R. B. (2005) Prion generation in vitro: Amyloid of Ure2p is infectious. *EMBO J. 24*, 3082–3092.
5. TerAvanesyan, A., Dagkesamanskaya, A. R., Kushnirov, V. V., and Smirnov, V. N. (1994) The SUP35 omnipotent suppressor gene is involved in the maintenance of the non-Mendelian determinant [psi+] in the yeast *Saccharomyces cerevisiae*. *Genetics 137*, 671–676.
6. Masison, D. C., and Wickner, R. B. (1995) Prion-inducing domain of yeast Ure2p and protease resistance of Ure2p in prion-containing cells. *Science 270*, 93–95.
7. Derkatch, I. L., Bradley, M. E., Zhou, P., Chernoff, Y. O., and Liebman, S. W. (1997) Genetic and environmental factors affecting the de novo appearance of the [PSI+] prion in *Saccharomyces cerevisiae*. *Genetics 147*, 507–519.
8. Sondheimer, N., and Lindquist, S. (2000) Rnq1: An epigenetic modifier of protein function in yeast. *Mol. Cell 5*, 163–172.
9. Derkatch, I. L., Bradley, M. E., Hong, J. Y., and Liebman, S. W. (2001) Prions affect the appearance of other prions: The story of [PIN]. *Cell 106*, 171–182.
10. Ross, E. D., Baxa, U., and Wickner, R. B. (2004) Scrambled prion domains form prions and amyloid. *Mol. Cell. Biol. 24*, 7206–7213.
11. Ross, E. D., Edskes, H. K., Terry, M. J., and Wickner, R. B. (2005) Primary sequence independence for prion formation. *Proc. Natl. Acad. Sci. U.S.A. 102*, 12825–12830.
12. Eanes, E. D., and Glenner, G. G. (1968) X-ray diffraction studies on amyloid filaments. *J. Histochem. Cytochem. 16*, 673–677.
13. Makin, O. S., and Serpell, L. C. (2005) Structures for amyloid fibers. *FEBS J. 272*, 5950–5961.
14. Lansbury, P. T., Jr., Costa, P. R., Griffiths, J. M., Simon, E. J., Auger, M., Halverson, K. J., Kocisko, D. A., Hendsch, Z. S., Ashburn, T. T., Spencer, R. G., et al. (1995) Structural model for the β-amyloid fibril based on interstrand alignment of an antiparallel-sheet comprising a C-terminal peptide. *Nat. Struct. Biol. 2*, 990–998.
15. Benzinger, T. L., Gregory, D. M., Burkoth, T. S., Miller-Auer, H., Lynn, D. G., Botto, R. E., and Meredith, S. C. (1998) Propagating structure of Alzheimer's β-amyloid(10–35) is parallel β-sheet with residues in exact register. *Proc. Natl. Acad. Sci. U.S.A. 95*, 13407–13412.
16. Gregory, D. M., Benzinger, T. L. S., Burkoth, T. S., Miller-Auer, H., Lynn, D. G., Meredith, S. C., and Botto, R. E. (1998) Dipolar recoupling NMR of biomolecular self-assemblies: Determining inter- and intrastrand distances in fibrilized Alzheimer's β-amyloid peptide. *Solid State Nucl. Magn. Reson. 13*, 149–166.
17. Burkoth, T. S., Benzinger, T. L. S., Urban, V., Morgan, D. M., Gregory, D. M., Thiyagarajan, P., Botto, R. E., Meredith, S. C., and Lynn, D. G. (2000) Structure of the β-amyloid(10–35) fibril. *J. Am. Chem. Soc. 122*, 7883–7889.
18. Antzutkin, O. N., Balbach, J. J., Leapman, R. D., Rizzo, N. W., Reed, J., and Tycko, R. (2000) Multiple quantum solid-state NMR indicates a parallel, not antiparallel, organization of β-sheets in Alzheimer's β-amyloid fibrils. *Proc. Natl. Acad. Sci. U.S.A. 97*, 13045–13050.
19. Petkova, A. T., Ishii, Y., Balbach, J. J., Antzutkin, O. N., Leapman, R. D., Delaglio, F., and Tycko, R. (2002) A structural model for Alzheimer's β-amyloid fibrils based on experimental constraints from solid state NMR. *Proc. Natl. Acad. Sci. U.S.A. 99*, 16742–16747.
20. Petkova, A. T., Yau, W. M., and Tycko, R. (2006) Experimental constraints on quaternary structure in Alzheimer's β-amyloid fibrils. *Biochemistry 45*, 498–512.
21. Jayasinghe, S. A., and Langen, R. (2004) Identifying structural features of fibrillar islet amyloid polypeptide using site-directed spin labeling. *J. Biol. Chem. 279*, 48420–48425.
22. Der-Sarkissian, A., Jao, C. C., Chen, J., and Langen, R. (2003) Structural organization of α-synuclein fibrils studied by site-directed spin labeling. *J. Biol. Chem. 278*, 37530–37535.
23. Luca, S., Yau, W.-M., Leapman, R., and Tycko, R. (2007) Peptide conformation and supramolecular organization in amylin fibrils: Constraints from solid-state NMR. *Biochemistry 46*, 13505–13522.
24. Cobb, N. J., Sonnichsen, F. D., Mchaourab, H., and Surewicz, W. K. (2007) Molecular architecture of human prion protein amyloid: A parallel, in-register β-structure. *Proc. Natl. Acad. Sci. U.S.A. 104*, 18946–18951.
25. Palmer, M. S., Dryden, A. J., Hughes, J. T., and Collinge, J. (1991) Homozygous prion protein genotype predisposes to sporadic Creutzfeldt-Jakob disease. *Nature 352*, 340–342.
26. Mead, S., Stumpf, M. P., Whitfield, J., Beck, J. A., Poulter, M., Campbell, T., Uphill, J. B., Goldstein, D., Alpers, M., Fisher, E. M., and Collinge, J. (2003) Balancing selection at the prion protein gene consistent with prehistoric kurulike epidemics. *Science 300*, 640–643.
27. Priola, S. A., Caughey, B., Race, R. E., and Chesebro, B. (1994) Heterologous PrP molecules interfere with accumulation of protease-resistant PrP in scrapie-infected murine neuroblastoma cells. *J. Virol. 68*, 4873–4878.
28. DePace, A. H., Santoso, A., Hillner, P., and Weissman, J. S. (1998) A critical role for amino-terminal glutamine/asparagine repeats in the formation and propagation of a yeast prion. *Cell 93*, 1241–1252.
29. Ross, E. D., Minton, A. P., and Wickner, R. B. (2005) Prion domains: Sequences, structures and interactions. *Nat. Cell Biol. 7*, 1039–1044.
30. Chan, J. C. C., Oyler, N. A., Yau, W.-M., and Tycko, R. (2005) Parallel β-sheets and polar zippers in amyloid fibrils formed by residues 10−39 of the yeast prion protein Ure2p. *Biochemistry 44*, 10669–10680.
31. Shewmaker, F., Wickner, R. B., and Tycko, R. (2006) Amyloid of the prion domain of Sup35p has an in-register parallel β-sheet structure. *Proc. Natl. Acad. Sci. U.S.A. 103*, 19754–19759.
32. Baxa, U., Wickner, R. B., Steven, A. C., Anderson, D., Marekov, L., Yau, W.-M., and Tycko, R. (2007) Characterization of β-sheet structure in Ure2p1-89 yeast prion fibrils by solid state nuclear magnetic resonance. *Biochemistry 46*, 13149–13162.
33. Taylor, K. L., Cheng, N., Williams, R. W., Steven, A. C., and Wickner, R. B. (1999) Prion domain initiation of amyloid formation in vitro from native Ure2p. *Science 283*, 1339–1343.
34. Pines, A., Gibby, M. G., and Waugh, J. S. (1973) Proton-Enhanced NMR of Dilute Spins in Solids. *J. Chem. Phys. 59*, 569–590.
35. Bennett, A. E., Rienstra, C. M., Auger, M., Lakshmi, K. V., and Griffin, R. G. (1995) Heteronuclear Decoupling in Rotating Solids. *J. Chem. Phys. 103*, 6951–6958.
36. Tycko, R. (2007) Symmetry-based constant-time homonuclear dipolar recoupling in solid-state NMR. *J. Chem. Phys. 126*, 064506.
37. Petkova, A. T., and Tycko, R. (2002) Sensitivity enhancement in structural measurements by solid state NMR through pulsed spin locking. *J. Magn. Reson. 155*, 293–299.
38. Saito, H. (1986) Conformation-dependent ^{13}C chemical shifts: A new means of conformational characterization as obtained by high-resolution solid-state ^{13}C NMR. *Magn. Reson. Chem. 24*, 825–852.
39. Wishart, D. S., Sykes, B. D., and Richards, F. M. (1991) Relationship between nuclear magnetic resonance chemical shift and protein secondary structure. *J. Mol. Biol. 222*, 311–333.
40. Balbach, J. J., Ishii, Y., Antzutkin, O. N., Leapman, R. D., Rizzo, N. W., Dyda, F., Reed, J., and Tycko, R. (2000) Amyloid fibril formation by Aβ16–22, a seven-residue fragment of the Alzheimer's β-amyloid peptide, and structural characterization by solid state NMR. *Biochemistry 39*, 13748–13759.
41. Wishart, D. S., Bigam, C. G., Holm, A., Hodges, R. S., and Sykes, B. D. (1995) H-1, C-13 and N-15 Random Coil NMR Chemical-Shifts of the Common Amino-Acids. 1. Investigations of Nearest-Neighbor Effects. *J. Biomol. NMR 5*, 67–81.

42. Kochneva-Pervukhova, N. V., Poznyakovski, A. I., Smirnov, V. N., and Ter-Avanesyan, M. D. (1998) C-terminal truncation of the Sup35 protein increases the frequency of de novo generation of a prion-based [PSI$^+$] determinant in *Saccharmyces cerevisiae*. *Curr. Genet. 34*, 146–151.
43. Liu, J.-J., Sondheimer, N., and Lindquist, S. (2002) Changes in the middle region of Sup35p profoundly alter the nature of epigenetic inheritance for the yeast prion [PSI+]. *Proc. Natl. Acad. Sci. U.S.A. 99*, 16446–16453.
44. Petkova, A. T., Buntkowsky, G., Dyda, F., Leapman, R. D., Yau, W. M., and Tycko, R. (2004) Solid state NMR reveals a pH-dependent antiparallel β-sheet registry in fibrils formed by a β-amyloid peptide. *J. Mol. Biol. 335*, 247–260.
45. Ritter, C., Maddelein, M. L., Siemer, A. B., Luhrs, T., Ernst, M., Meier, B. H., Saupe, S. J., and Riek, R. (2005) Correlation of structural elements and infectivity of the HET-s prion. *Nature 435*, 844–848.
46. Siemer, A. B., Ritter, C., Steinmetz, M. O., Ernst, M., Riek, R., and Meier, B. H. (2006) ^{13}C, ^{15}N resonance assignment of parts of the HET-s prion protein in its amyloid form. *J. Biomol. NMR 34*, 75–87.
47. Johnson, S. M., Wiseman, R. L., Sekijima, Y., Green, N. S., Adamski-Werner, S. L., and Kelly, J. W. (2005) Native state kinetic stabilization as a strategy to ameliorate protein misfolding diseases: A focus on the transthyretin amyloidoses. *Acc. Chem. Res. 38*, 911–921.
48. Mallucci, G., Dickinson, A., Linehan, J., Klohn, P. C., Brandner, S., and Collinge, J. (2003) Depleting neuronal PrP in prion infection prevents disease and reverses spongiosis. *Science 302*, 871–874.
49. Leinala, E. K., Davies, P. L., Doucet, D., Tyshenko, M. G., Walker, V. K., and Jia, Z. (2002) β-Helical antifreeze protein isoform with increased activity: Structural and functional insights. *J. Biol. Chem. 277*, 33349–33352.

BI7024589